Research Project Report [1]

Mathematical Model of Nuclear-factor-kappa-B through Erb4 signalling

Carlos Andres Mariscal Melgar

Student I.D. 200692669

Supervisor: [Dr Steven Webb]

Internal Assessor: [Prof David MacEwan]

Strand: [Drug Safety]

Word Count: [3981]

Mathematical Model of Nuclear-factor-kappa-B through Erb4 signalling

Abstract:

Nuclear factor kappa B (NFkB) is a critical regulator of the cellular response against cellular stress and infection. Ordinary differential equations (ODE) kinetics based mathematical model describing the NFkB pathway *in silico was created and, m*olecular events included: Receptor tyrosine-protein kinase (Erb4) activation that leads to phosphoinositide-3-kinase (PI3K) mediated Protein kinase B (AKT) activation. AKT induced IkB kinase (IKK) is critical for NFkB release from nuclear factor kappa light polypeptide gene enhancer in B-Cells inhibitor, alpha (IkBa) sequestration and culminating in NFkB nuclear translocation for nuclear transcriptional regulation leading to negative feedback and oscillatory behaviour of the system.

Introduction

The purpose of this project is to build an *in silico* mathematical model of the Nuclear-Factor-kappa-B (NFkB) signalling pathway, onto which BTK modules can be incorporated to optimize analysis of BTK inhibitors such as Ibrutinib. Ultimately the aim is to have a fully working *in silico* model capable of simulating with relative accuracy KO and wild type signalling responses.

Ibrutinib is a drug that has been recently approved for phase two clinical trials, it acts on the Bruton's Tyrosine Kinase as an inhibitor (3) The drug shows potential through its ability to inhibit this pathway that feeds downstream to numerous inflammatory proliferative pathways (4). Ibrutinib is particularly well tolerated by patients and it is this characteristic relatively lower adverse drug reaction and a good safety profile (3), that makes this such a desirable drug for B-cell malignancies, namely Chronic Myeloid Leukaemia (CML), B-cell non-Hodgkin lymphoma, diffuse large cell lymphomas or mantle cell lymphoma (3-5) and with possible potential to treat autoimmune disorders such as lupus or rheumatoid arthritis (4, 5).

NFkB is the generic name used for a family of evolutionarily conserved transcription factors that function through dimerization and ultimately regulate genes that are involved in immunity, inflammation, cell survival, proliferation, differentiation and, apoptosis (6, 7). Because chronic inflammatory diseases and cancer often have NFkB involvement and, since NFkB is a key regulator in oncogenesis by promoting proliferation and inhibiting apoptosis (8), NFkB and its associated proteins have become desirable targets for the development of novel drugs and therapeutics (3, 5, 8). NFkB belongs to the Rel family of proteins which encompasses 5 different mammalian proteins namely: p65, C-Rel, RelB, NFkB1 (p50/p105) and NFkB2 (p52/100) (6). Synthesis of these proteins occurs with p105 and p100 being synthesised as large precursors to p50 and p52 with p65, C-Rel and, RelB being synthesised in a mature form.

The NFkB pathway can be targeted upstream or downstream with the ultimate aim of changing the flux of information to obtain the desired response, thus allowing all associated pathways to be potential drug targets (3). NFkB can be activated by numerous pathways, the most commonly associated factor that induces NFkB activity are the tumour necrosis factor-alpha (TNF-α) (9). Although the tumour necrosis factor superfamily is all able to induce the NFkB pathway (9) and can also be activated by interleukin-1 (IL-1) (10) as well by-products of bacterial and viral infections (6).In this particular instance, NFkB activation was modelled through a TNF-α analogue in AKT- PIP2.

NFkB activation involves a signal dependant activation of the IkappaB kinase (IKK)(7, 9). The IKK complex is composed of three subunits IKKα, KKβ and, IKKγ (6). IKKα and IKKβ are the catalytic subunits of the IKK complex whereas IKKγ is the regulatory subunit. Catalytic activity by IKKβ is essential for the activation of the pathway, which occurs on serine residues 19 and 21 of the N-terminal in IkBb and serine residues 32 and 36 for IkBa) (6, 9) IKK activation is therefore essential for NFkB activation, since activation of IKK can occur through the same stimuli that activates NFkB, such as inflammatory cytokines, and by-products of microbial, fungal and viral infections (6). Once NFkB is activated through phosphorylation of the IkB inhibitory protein, IkBa is ubiquitinated and primed for destruction by the proteasome (9, 11) and, activated NFkB is translocated into the nucleus where it can regulate transcription (11) and, leading to a physiological response such as a immune response (6).

Methods

Systems Biology is an emergent field in the biosciences. Coined earlier in the 20th century, the meaning now encompasses a broad interdisciplinary field where engineering, mathematics and, computer science collide with experimental biology. System biology as used in this work as the representation and modelling of complex biological interactions in the form of mathematical Ordinary Differential Equations (ODEs).

Matlab is one of the most widely used numerical platforms in science and engineering,

In order to model the system Mathworks Simbiology package was used.

Simbiology is a specialised Matlab toolbox, enabling pharmacokinetic/pharmacodynamic and signal transduction kinetic data modelling by providing graphical and programmatic tools. Simbiology was chosen to model, simulate and analyse the dynamic biological system in this rotation.

Signal transduction and kinetic data can be specified for the type of reaction occurring through the use of mathematical representation of the reactions.

Reactions are represented in the format X <-> Y and can be rearranged using the built in block diagram editor view. Simbiology is also able to use Matlab's diverse ODE solvers and stochastic simulation capabilities and allows for cross platform functionality by being able to import and export SBML files.

In order to model the signal transduction pathway, mathematical representations of the biological events were used.

Signal transduction pathways occur mostly through two mechanisms:

Protein-protein interactions that can be represented through Mass action kinetics or enzyme dependent reactions, often simplified as Michaelis Menten kinetics, such as protein phosphorylation and de-phosphorylation and, protein degradation and production (12).

For this particular model Mass Action was assumed for most reactions, Michaelis- Menten kinetics for enzyme catalysed reactions and, hill functions for multi-substrate/multi-binding-site enzyme catalysed reactions.

Kinetic laws:

Mass action- The law of mass action states that the reaction rate is proportional to the probability of a collision of the reactants, which is in turn proportional to the concentration of the reactants.

Assuming a reversible reaction of two substrates S_1 and S_2

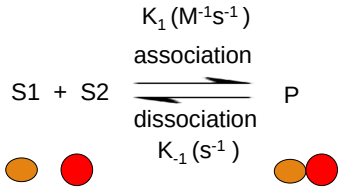

The net reaction rate is given by the rate of the forward reaction minus the rate of the backward reaction:

$$\frac{d[P]}{dt} = -\frac{d[S_1]}{dt} = -\frac{d[S_2]}{dt} = k_1[S_1][S_2] - k_{-1}[P]$$

In which k_1 and k_{-1} are kinetic, or rate, constants and, [.] denotes concentration.

Michaelis-Menten kinetics- First described by Leonor Michaelis and Maud Menten (13)

Michaelis-Menten equation for an isolated reaction:

$S \xrightarrow{E} P$: Substrate S is transformed into product P through a catalysed reaction using enzyme E (where S can be a inactive/dephosphorylated form of a protein, P can be an activated/phosphorylated form of the protein and E is the enzyme or kinase catalysing the reaction). For an isolated system, the rate of production of P (dP/dt) is proportional to the rate of consumption of S (dS/dt) and therefore the rate of reaction (v) can be written as follows:

$$v = \frac{d[P]}{dt} = -\frac{d[S]}{dt} = \frac{V_{max}[S]}{K_M + [S]}$$

Where K_M (μM) is the Michaelis-Menten dissociation constant and V_{max} (1/s) is the maximum velocity rate. A full derivation of this formula can be expressed as follows. Consider the following enzyme-substrate reaction.

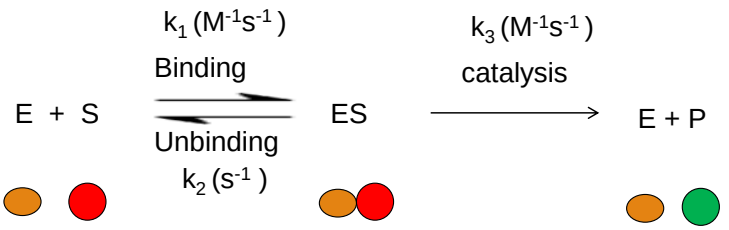

Then, according to the Law of Mass Action, we have

$$\frac{d[E]}{dt} = -k1[E][S] + k3[ES] + k2[ES]$$

$$\frac{d[ES]}{dt} = k1[E][S] - k2[ES] - k3[ES]$$

and

$$\frac{d[P]}{dt} = k3[ES]$$

A quasi-steady state assumption is then assumed. This quasi steady state assumption was first stipulated by Briggs and Haldane in 1925 (14) and assumes the following:

$$\frac{dES}{dt} = 0 = \frac{dE}{dt}$$

Therefore:

$$0 = +k1[E][S] - k3[ES] - k2[ES]$$

With a constant number of enzyme

$$[E]_0 = [E] + [ES]$$

This becomes

$$0 = k1([E]_0 - [ES])[S] - (k2 + k3)[ES]$$

Rearranging for [ES] gives

$$[ES] = \frac{[E]_0[S]}{\frac{k2 + k3}{k1} + [S]}$$

Substituting into the d[p]/d[t] equation then gives

$$\frac{d[P]}{dt} = \frac{(k3[E]_0)[S]}{[S]+K_M}$$ Where $$(k3[E]_0) = Vmax$$

Namely

$$\frac{d[P]}{dt} = \frac{Vmax[S]}{[S]+K_M}$$

Hill kinetics: First proposed by Barcroft and Hill (15) in order to explain how haemoglobin O_2 saturation curves generated a sigmoidal curve and proposed the use of an exponential power to produce the sigmoidal curve with theoretical basis on multiple subunit binding.

Various molecular mechanisms have been stated to explain the sigmoidal curves generated with Hill kinetics, which often are representative of biomolecular processes such as transcription(16, 17). Molecular mechanisms that have been stipulated in order to explain this behaviour include: cooperative binding sites (15) multimer formation(17), competition between a repressor and an activator on a given binding site (16) and positive-feedback loop models (18).Sigmoid responses are therefore mostly seen in multimeric systems with cooperative interactions. Binding at one site results in a change in the binding affinities of the remaining sites and therefore Hill kinetics can present limitations when assessing relative contributions of each cooperative molecule (19).

Hill equation derivation-

Assume that an enzyme (E) binds, for example, simultaneously with multiple (n) substrates (S), namely:

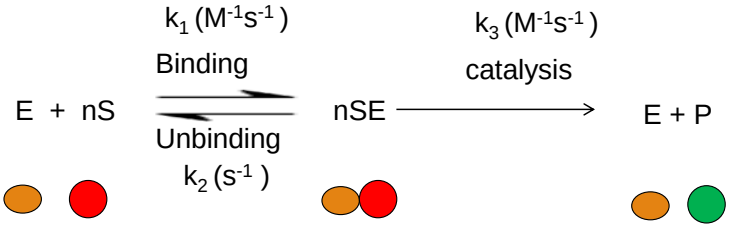

Following the same quasi-steady state argument stipulated by Briggs and Haldane (14), namely that d[nSE]/dt=0 , and again assuming a constant number of enzyme ($[E]_0$), one can obtain

$$\frac{d[P]}{dt} = \frac{(k_3[E]_0 S^n)}{\frac{k_2 + k_3}{k_1} + S^n} = \frac{Vmax + S^n}{K_M + S^n}$$

Where n is often described as the Hill coefficient.

In order to construct the mathematical model, during the literature search different elements from pre-existing mathematical models were analysed

and chosen based on their representation of the pathway.

The following models were used in order to construct the mathematical model.

Ashall model (2) –

Table 1 Modular components description of the Ashall model that was used in the final model.

	Biological event	Parameter value	Units	Type of Reaction	Reaction Kinetics
1	A20 induced IKKi return to IKKn	kp= 6.0E-4 ; kbA20= 0.0018	kp= uM^2/s ; kbA20= uM/s	Mass Action	kp*IKKi*(kbA20/(kbA20+Cytoplasm.A20*AKT_PIP2))
2	AKT-PIP2 mediated IKKn activation	2.50E-03	1/(uM*s)	Mass Action	k1*Cytoplasm.IKKn*Cytoplasm.AKT_PIP2

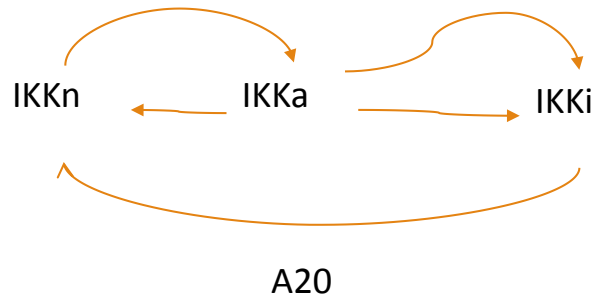

Figure 1 Diagrammatic representation of the Ashall model's neutral state IKK and the A20 mediated IKKi -> IKKn induction

This part of the Ashall model was implemented in the model as it contains a neutral state of IKK, that cross-talks with the inactive state of IKK through A20 presence after nNFkB transcription.

Gong (20) –

Table 2 Modular components description of the Gong model that was used in the final model

	Biological event	Parameter value	Units	Type of Reaction	Reaction Kinetics
1	PI3K induced PIP2 phosphorylation to PIP3	3.00E-06	1/molecule*minute	Mass Action	k3*PI3Ka*PIP2

2	PTEN induction of transcription by P53 activity	k5g=0.064 K1=0.016	k5g= 1/s ; K1=1/(uM*s)	Hill Kinetics	k5g*Cytoplasm.P53^3/ (K1^3+Cytoplasm.P53^3)
3	PTEN degradation	0.006	1/s	Mass Action	d5*Cytoplasm.PTEN
4	nNFkB induced P53 transcription	k9g= 9.6E-7 ; kp=4.0E-15 ; Kn=0.04	k9g= uM/s ; kp= uM/s ; Kn= uM	Michaelis-Menten	k9g+k9p*nucleus.nNFkB/ (Kn+nucleus.nNFkB)
5	P53 degradation	d9p=6.0E-7 ; d9= 0.012	d9p= uM/s ; d9= 1/s	Michaelis-Menten	(d9+d9p*Cytoplasm.MDM2p)* Cytoplasm.P53
6	P53 induced MDM2t transcription	k6g=4.267E-7 ; K1g=0.064	k6g= uM/s ; K1g= uM	Hill Kinetics	k6g*Cytoplasm.P53^3/ (K1g^3+Cytoplasm.P53^3)
7	MDM2t degradation	0.018	1/s	Mass Action	d6*Cytoplasm.MDM2t
8	MDM2t induced MDM2 production	0.5	1/s	Mass Action	k7g*Cytoplasm.MDM2t
9	MDM2 degradation	2.33E-04	1/s	Mass Action	d7*Cytoplasm.MDM2
10	AKT_PIP2 induced MDM2 phosphorylation	k8g=3.2E-13 ; d8= 5.0E-4	k8g= 1/(uM*s) ; d8= 1/s	Mass Action	k8g*Cytoplasm.AKT_PIP2* Cytoplasm.MDM2
11	MDM2p dephosphorylation	5.00E-04		Mass Action	d8*Cytoplasm.MDM2p
12	MDM2p degradation	2.17E-04	1/s	Mass Action	d8p*Cytoplasm.MDM2p

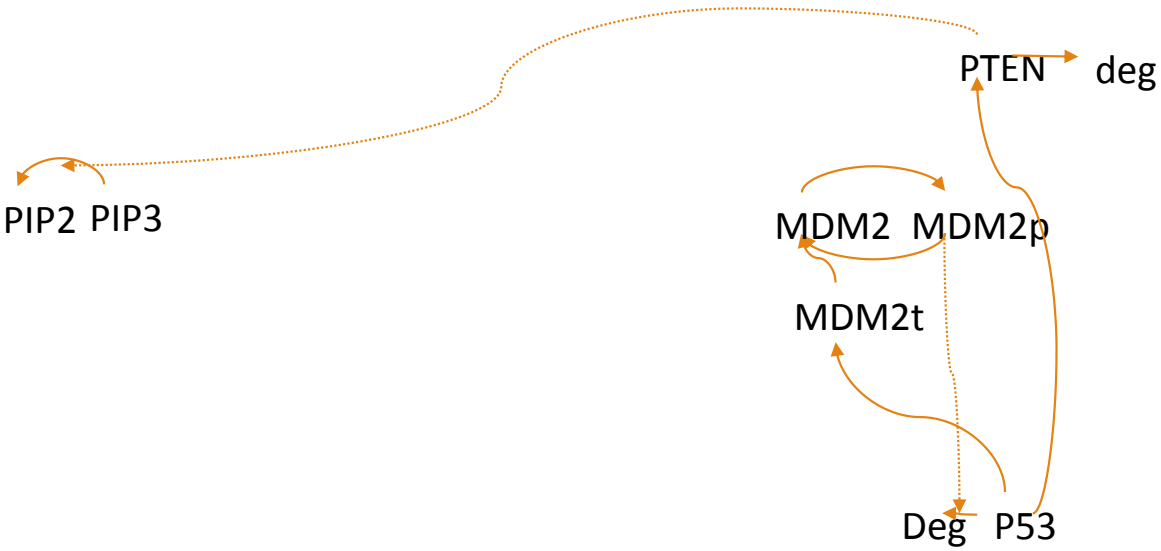

Figure 2 Diagrammatic representation of the Gong model P53 induced PIP3 de-phosphorylation

This part of the Gong model was used because nNFkB induced P53 transcription provided a negative feedback loop for the model through the PIP3 de-phosphorylation step.

Lipniacky (11) –

Table 3 Modular components description of the Lipniacky model that was used in the final model.

	Biological event	Parameter value	Units	Type of Reaction
1	IKK-IκBα association	0.2	1/(uM*s)	Mass action
2	IκBα-NF-κB association	0.5	1/(uM*s)	Mass action
3	IKK-IκBα:NF-κB association	1	1/(uM*s)	Mass action
4	IKK:IκBα catalysis	0.1	1/s	Mass action
5	IKK:IκBα:NF-κB catalysis	0.1	1/s	Mass action
6	IκB degradation (free)	0.0001	1/s	Mass action
7	IκB degradation (complexed)	0.00002	1/s	Mass action
8	A20 degradation	0.0003	1/s	Mass action
9	NF-κB-inducible IκBα mRNA synthesis	5*10^-7	1/(uM*s)	Mass action
10	NF-κB-inducible A20 mRNA synthesis	5*10^-7	1/(uM*s)	Mass action
11	Constitutive IκBα mRNA synthesis	0	μM/s	Mass action
12	Constitutive A20 mRNA synthesis	0	μM/s	Mass action
13	IκBα mRNA degradation	0.0004	1/s	Mass action

14	A20 mRNA degradation	0.0004	1/s	Mass action
15	IκBα mRNA translation	0.5	1/s	Mass action
16	A20 mRNA translation	0.5	1/s	Mass action
17	IKKn activation caused by TNFα	0.0025	1/s	Mass action
18	IKKa inactivation caused by A20	0.1	1/s	Mass action
19	IKKa spontanouous inactivation	0.0015	1/s	Mass action
20	IKKn production rate	0.000025	1/s	Mass action
21	Degradation of IKKa,IKKn & IKKi	0.000125	1/s	Mass action
22	NF-κB nuclear import	0.0025	1/s	Mass action
23	nIκBα:nNF-κB nuclear export	0.01	1/s	Mass action
24	IκBα nuclear import (including IκBα ubiquitination & degradation)	0.001	1/s	Mass action
25	IκBα nuclear export	0.0005	1/s	Mass action
26	C:N volume ratio	kv	5	
27	Total NF-κB conc. (initial as IκBα·NFκB)	NF	0.06 V μM	

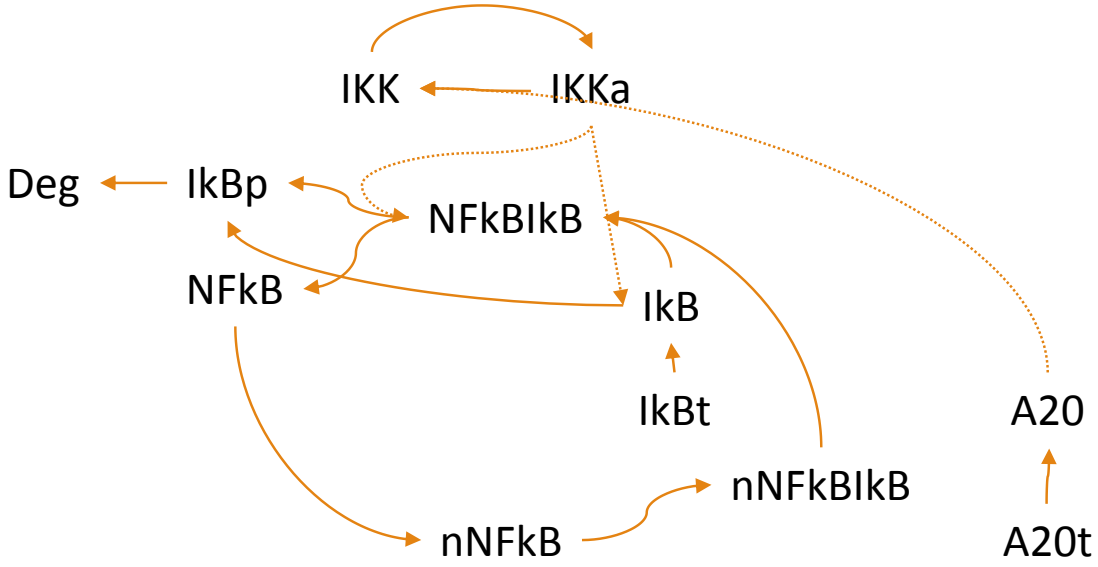

Figure 3 Diagrammatic representation of the Lipniacky model.

The Lipniacky model describes crucial elements of the NFkB pathway, namely IKK activation dependence of the pathway. NFkB located in the cytosol is found as a complex with the inhibitory protein IkBa, IKK activation then phosphorylates IkBa resulting in dissociation and degradation. Free NFkB then is translocated into the nucleus where it can regulate transcription.

Hatakeyama (21) –

Table 4 Modular components description of the Hatakeyama model used in the final model

	Biological event	Parameter value	Units	Type of Reaction	Reaction Kinetics
1f	R + HRG -> R-HRG	0.0012*10^-3	1/(uM*s)	Mass Action	k1*[ErbB4-R]*HRG
1r	R-HRG -> R + HRG	0.00076 ; 1/s	1/s	Mass Action	[k1']*R_HRG
2f	R-HRG -> R-HRG2	0.01*10^-3 ; 1/(uM*s)	1/(uM*s)	Mass Action	k2*R_HRG^2
2r	R-HRG2 -> R-HRG	0.1 ; 1/s	1/s	Mass Action	[k'2]*R_HRG2
3f	R-HRG2 -> RP	1 ; 1/s	1/s	Mass Action	k3*R_HRG2
3r	RP -> R-HRG2	0.01 ; 1/s	1/s	Mass Action	[k3']*RP

4f	RP -> R-HRG2	V4= 62.5 *10^-3 ; 1/(uM*s) ; K4= *10^-3 ; uM	V4= 1/(uM*s) K4= uM	Michaelis-Menten	V4*RP/(K4+RP)
5f	RP -> null	0.001 ; 1/s	1/s	Mass Action	k34*RP
6f	PI3K + RP -> R-PI3K	0.1*10^-3 ; 1/(uM*s)	1/(uM*s)	Mass Action	k23*PI3K*RP
6r	R-PI3K -> PI3K + RP	2 ; 1/s	1/s	Mass Action	[k23']*R_PI3K
7f	R-PI3K -> R-PI3K*	9.85 ; 1/s	1/s	Mass Action	k24*R_PI3K
7r	R-PI3K* -> R-PI3K	0.0985 ; 1/s	1/s	Mass Action	[k24']*[R_PI3K*]
8f	R-PI3K* -> RP + PI3K*	45.8 ; 1/s	1/s	Mass Action	k25*[R_PI3K*]
8r	RP + PI3K* -> R-PI3K*	0.047 *10^-3 ; 1/(uM*s)	1/(uM*s)	Michaelis-Menten	[k25']*[PI3K*]*RP
9f	PI3K* -> PI3K	V26= 2620 *10^-3 ; 1/(uM*s) ; K26= 3680 *10^-3 ; uM	V26= 1/(uM*s) ; K26= uM	Michaelis-Menten	V26*[PI3K*]/(K26+[PI3K*])
10f	PI3K* induces PIP2 -> PIP3	V 28 = 17000 ; K 28 = 9.02	1/(uM*s)	Mass Action	V 28[PIP3]/(K 28 +[PIP3])
10r	PI3K* induces PIP2 -> PIP3	k27=16.9 *10^-3 ; 1/(uM*s) ; K27=39.1 ; 1/s	k27= 1/(uM*s) K27=1/s	Michaelis-Menten	(k27*[PI3K*]*PI)/(K27+PI)
11f	PIP3 + AKT -> AKT-PIP3	507*10^-3 ; 1/(uM*s)	1/(uM*s)	Mass Action	k29*PIP3*AKT
11r	AKT-PIP3 -> PIP3 + AKT	234 ; 1/s	1/s	Mass Action	k_29*AKT_PIP3
12f	PDK induces AKT-PIP3 -> AKT- PIP	V30=20000 *10^-3 ; 1/(uM*s) ;K30=80000*10^-3 ; uM	V30=1/(uM*s) K3-1/(uM*s)	Michaelis-Menten	(V30*AKT_PIP3)/ (K30+AKT_PIP3)
13f	P P2A induces AKT-PIP -> AKT-PIP3	k31= 0.107; 1/s ;K31=4.35 *10^-3 ; uM	k31= 1/s K31= uM	Michaelis-Menten	(k31*PP2A*AKT_PIP)/ (K31+AKT_PIP3)
14f	PDK induces AKT-PIP -> AKT-PIP2	V32=20000*10^-3 ; 1/(uM*s) ;K32=80000 *10^-3 ; uM	V32= 1/(uM*s) K32= uM	Michaelis-Menten	(V32*AKT_PIP)/ (K32+AKT_PIP)
15f	PP2A induces AKT-PIP2 -> AKT-PIP	k33=0.211; 1/s K33=12*10^-3 ; uM	k33= 1/s K33= uM	Michaelis-Menten	(k31*PP2A*AKT_PIP)/ (K31+AKT_PIP3)

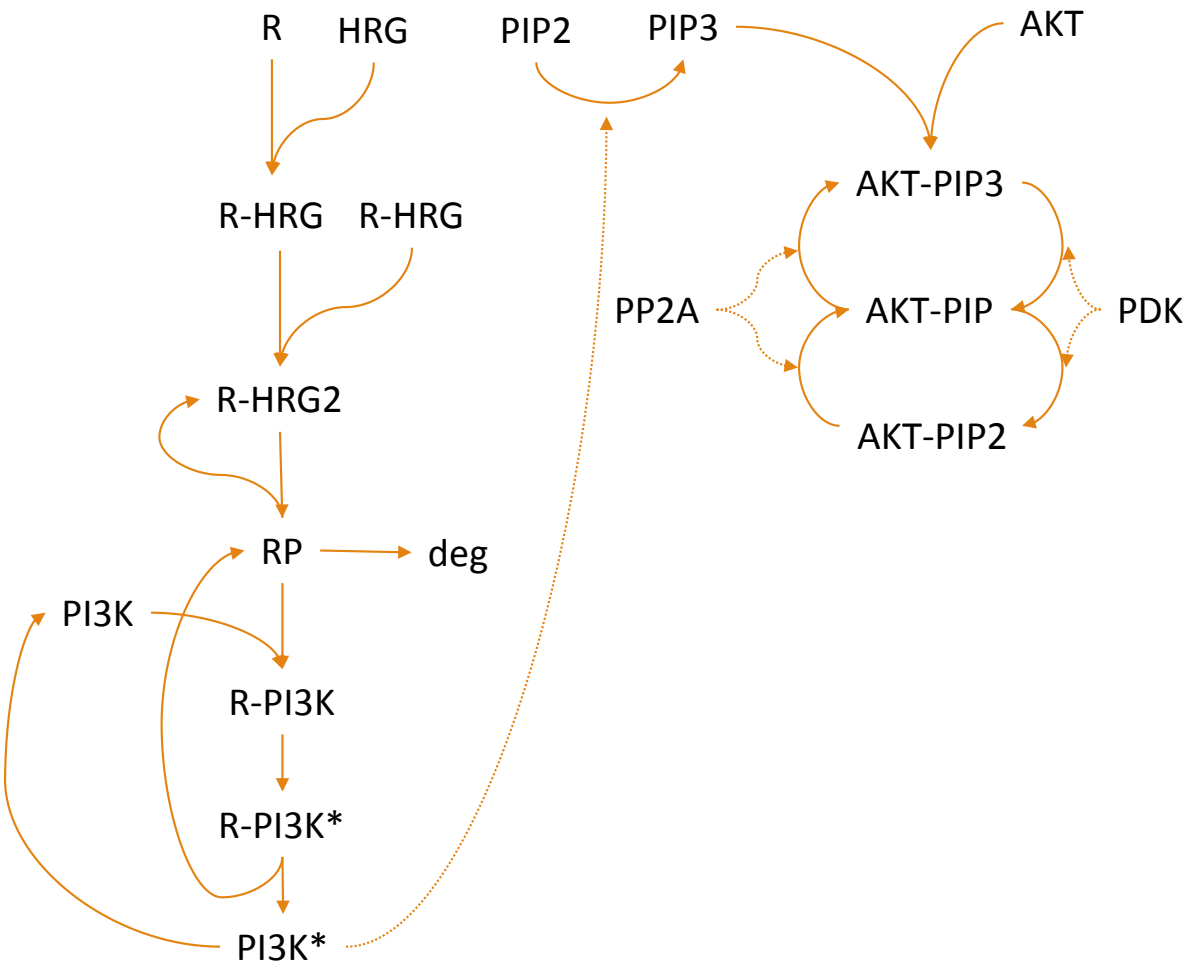

Figure 4 Diagrammatic representation of the Hatakeyama model

In order to link into the BTK pathway we incorporated elements from the hatakeyama model, the presence of the ErB4 receptor, which undergoes dimerization prior to phosphorylation, activating PI3K.

Activated PI3K then phosphorylates PIP2 which in turn binds with AKT culminating in AKT-PIP2 which is an active form able to feed into the combined model through IKK interaction.

Combined model (2, 11, 20, 21) –

Table 5 Description of the final combined model for the NFkB pathway. Highlighted in red are parameters modified based on sensitivity analysis.

	Parameter Values	Units	Reaction description	Type of Reaction	Reaction kinetics
1f	0.0012*10^-3	1/(uM*s)	R + HRG -> R-HRG	Mass Action	k1*[ErbB4-R]*HRG
1r	0.00076 ; 1/s	1/s	R-HRG -> R + HRG	Mass Action	[k1']*R_HRG
2f	0.01*10^-3 ; 1/(uM*s)	1/(uM*s)	R-HRG -> R-HRG2	Mass Action	k2*R_HRG^2
2r	0.1 ; 1/s	1/s	R-HRG2 -> R-HRG	Mass Action	[k'2]*R_HRG2
3f	1 ; 1/s	1/s	R-HRG2 -> RP	Mass Action	k3*R_HRG2
3r	0.01 ; 1/s	1/s	RP -> R-HRG2	Mass Action	[k3']*RP
4f	V4= 62.5 *10^-3 ; 1/(uM*s) ; K4= *10^-3 ; uM	V4= 1/(uM*s) K4= uM	RP -> R-HRG2	Michaelis-Menten	V4*RP/(K4+RP)
5f	0.001 ; 1/s	1/s	RP -> null	Mass Action	k34*RP
6f	0.1*10^-3 ; 1/(uM*s)	1/(uM*s)	PI3K + RP -> R-PI3K	Mass Action	k23*PI3K*RP
6r	2 ; 1/s	1/s	R-PI3K -> PI3K + RP	Mass Action	[k23']*R_PI3K
7f	9.85 ; 1/s	1/s	R-PI3K -> R-PI3K*	Mass Action	k24*R_PI3K
7r	0.0985 ; 1/s	1/s	R-PI3K* -> R-PI3K	Mass Action	[k24']*[R_PI3K*]
8f	45.8 ; 1/s	1/s	R-PI3K* -> RP + PI3K*	Mass Action	k25*[R_PI3K*]
8r	0.047 *10^-3 ; 1/(uM*s)	1/(uM*s)	RP + PI3K* -> R-PI3K*	Michaelis-Menten	[k25']*[PI3K*]*RP
9f	V26= 2620 *10^-3 ; 1/(uM*s) ; K26= 3680 *10^-3 ; uM	V26= 1/(uM*s) ; K26= uM	PI3K* -> PI3K	Michaelis-Menten	V26*[PI3K*]/(K26+[PI3K*])
10f	0.000003 ; 1/molecule*minute V 3e-6*cscale*(60*10^-3) =225 *10^-3 ; 1/(uM*s)	1/(uM*s)	PI3K* induces PIP2 -> PIP3	Mass Action	k3*PI3Ka*PIP2
10r	k27=16.9 *10^-3 ; 1/(uM*s) ;	k27= 1/(uM*s) K27=1/s	PI3K* induces PIP2 -> PIP3	Michaelis-Menten	(k27*[PI3K*]*PI)/(K27+PI)

	K27=39.1 ; 1/s				
11f	507*10^-3 ; 1/(uM*s)	1/(uM*s)	PIP3 + AKT -> AKT-PIP3	Mass Action	k29*PIP3*AKT
11r	234 ; 1/s	1/s	AKT-PIP3 -> PIP3 + AKT	Mass Action	k_29*AKT_PIP3
12f	V30=20000 *10^-3 ; 1/(uM*s) ;K30=80000* 10^-3 ; uM	V30=1/(u M*s) K3- 1/(uM*s)	PDK induces AKT-PIP3 -> AKT- PIP	Michael is-Menten	(V30*AKT_PIP3)/(K30+AKT_PIP3)
13f	k3 1=0.107; 1/s ;K31=4.35 *10^-3 ; uM	k31= 1/s K31= uM	P P2A induces AKT-PIP -> AKT-PIP3	Michael is-Menten	(k31*PP2A*AKT_PIP)/(K31+AKT_ PIP3)
14f	V32=20000*1 0^-3 ; 1/(uM*s) ;K32=80000 *10^-3 ; uM	V32= 1/(uM*s) K32= uM	PDK induces AKT-PIP -> AKT-PIP2	Michael is-Menten	(V32*AKT_PIP)/(K32+AKT_PIP)
15f	k33=0.211; 1/s K33=12*10^-3 ; uM	k33= 1/s K33= uM	PP2A induces AKT-PIP2 -> AKT-PIP	Michael is-Menten	(k31*PP2A*AKT_PIP)/(K31+AKT_ PIP3)
16f	2.50E-03	1/(uM*s)	AKT-PIP2 activates IKKn -> IKKa	Mass Action	k1*Cytoplasm.IKKn*Cytoplasm.AK T_PIP2
17f	1.25E-04	1/s	IKKn -> deg2	Mass Action	k2*Cytoplasm.IKKn
18f	k4= 0.1 ; k5g=0.064	k4= 1/(uM*s) ; k5g= uM	IKKa + A20 -> IKKi + A20	Mass Action	k5*Cytoplasm.IKKa+k4*Cytoplas m.IKKa*Cytoplasm.A20
19f	1.25E-04	1/s	IKKi -> deg	Mass Action	k11*Cytoplasm.IKKi
20f	0.2	1/(uM*s)	IkBa + IKKa -> IKKa_IkBa	Mass Action	k7*Cytoplasm.IKKa*Cytoplasm.Ik Ba
21f	0.1	1/s	IKKa_IkBa -> IKKa	Mass Action	k8*Cytoplasm.IKKa_IkBa
22f	1.25E-04	1/s	IKKa -> deg	Mass Action	k6*Cytoplasm.IKKa
23f	5.3E-4	1/s	(IKKa Induced)NFk B_IkBa + IKKa -> NFkB + IKKa	Mass Action	k12*Cytoplasm.NFkB_IkBa
24f	0.1	1/s	NFkB_IkBa_I KKa -> NFkB + IKKa	Mass Action	k10*Cytoplasm.NFkB_IkBa_IKKa
25f	1	1/(uM*s)	IKKa + NFkB_IkBa -> NFkB_IkBa_I	Mass Action	k9*Cytoplasm.IKKa*Cytoplasm.NF kB_IkBa

			KKa		
26f	18.4	1/(uM*s)	IkBa + NFkB -> NFkB_IkBa	Mass Action	kf13*Cytoplasm.NFkB*Cytoplasm.IkBa
26r	18.4	1/s	NFkB_IkBa -> IkBa + NFkB	Mass Action	kr13*Cytoplasm.NFkB_IkBa
27f	1.00E-04	1/s	IkBa -> deg	Mass Action	k21*Cytoplasm.IkBa
28f	0.001	1/s	IkBa -> 5 nIkBa	Mass Action	kf23*Cytoplasm.IkBa
28r	5.00E-04	1/s	5 nIkBa -> IkBa	Mass Action	kr23*nucleus.nIkBa
29f	0.0025	1/s	NFkB -> 5 nNFkB	Mass Action	kf15*Cytoplasm.NFkB
29r	0	1/s	5 nNFkB -> NFkB	Mass Action	kr15*nucleus.nNFkB
30f	18.4	1/(uM*s)	nNFkB + nIkBa -> nNFkB_nIkBa	Mass Action	kf14*nucleus.nNFkB*nucleus.nIkBa
30r	0	1/s	nNFkB_nIkBa -> nNFkB + nIkBa	Mass Action	kr14*nucleus.nNFkB_nIkBa
31f	0.01	1/s	5 nNFkB_nIkBa -> NFkB_IkBa	Mass Action	kf28*nucleus.nNFkB_nIkBa
31r	0	1/s	NFkB_IkBa -> 5 nNFkB_nIkBa	Mass Action	kr28*Cytoplasm.NFkB_IkBa
32f	3.4E-7	1/s	nNFkB + nIkBa -> mRNAIkBa + nNFkB	Mass Action	k26*nucleus.nNFkB
33f	4.00E-04	1/s	mRNAA20 -> deg	Mass Action	k17*Cytoplasm.mRNAA20
34f	0.5	1/s	mRNAA20 -> A20 + mRNAA20	Mass Action	k16*Cytoplasm.mRNAA20
35f	3.00E-04	1/s	A20 -> deg	Mass Action	k18*Cytoplasm.A20
36f	4.00E-04	1/s	mRNAIkBa -> deg	Mass Action	k27*Cytoplasm.mRNAIkBa
37f	0.5	1/s	mRNAIkBa -> IkBa + mRNAIkBa	Mass Action	k22*Cytoplasm.mRNAIkBa
38f	kp= 6.0E-4 ; kbA20= 0.0018	kp= uM^2/s ; kbA20= uM/s	IKKi -> IKKn	Mass Action	kp*IKKi*(kbA20/(kbA20+Cytoplasm.A20*AKT_PIP2))
39f	k5g=0.064 K1=0.016	k5g= 1/s ; K1=1/(u	null -> PTEN	Hill Kinetics	k5g*Cytoplasm.P53^3/(K1^3+Cytoplasm.P53^3)

		M*s)			
40f	0.006	1/s	PTEN -> null	Mass Action	d5*Cytoplasm.PTEN
41f	k9g= 9.6E-7 ; kp=4.0E-15 ; Kn=0.04	k9g= uM/s ; kp= uM/s ; Kn= uM	nNFkB -> .P53 + nNFkB	Michaelis-Menten	k9g+k9p*nucleus.nNFkB/(Kn+nucleus.nNFkB)
42f	d9p=6.0E-7 ; d9= 0.012	d9p= uM/s ; d9= 1/s	P53 -> null	Michaelis-Menten	(d9+d9p*Cytoplasm.MDM2p)*Cytoplasm.P53
43f	k6g=4.267E-7 ; K1g=0.064	k6g= uM/s ; K1g= uM	P53 -> MDM2t + P53	Hill Kinetics	k6g*Cytoplasm.P53^3/(K1g^3+Cytoplasm.P53^3)
44f	0.018	1/s	MDM2t -> null	Mass Action	d6*Cytoplasm.MDM2t
45f	0.5	1/s	MDM2t -> MDM2 + MDM2t	Mass Action	k7g*Cytoplasm.MDM2t
46f	2.33E-04	1/s	MDM2 -> null	Mass Action	d7*Cytoplasm.MDM2
47f	k8g=3.2E-13 ; d8= 5.0E-4	k8g= 1/(uM*s) ; d8= 1/s	MDM2 -> MDM2p	Mass Action	k8g*Cytoplasm.AKT_PIP2*Cytoplasm.MDM2
48f	5.0E-4	1/s	MDM2p -> MDM2	Mass Action	d8*Cytoplasm.MDM2p
48r	2.17E-04	1/s	MDM2p -> null	Mass Action	d8p*Cytoplasm.MDM2p

All do the models shown were then combined into a composite model of NFkB signalling, linking the Hatakeyama model through PIP2 phosphorylation, Akt_pip3 part of the pathway being used as a TNF-alpha analogue to mediate IKK activation whilst also interacting with the MDM2 phosphorylation step, The neutral state was added from the Ashall model and from the Lipniacky model a increased feedback generated by increased transcription of P53.

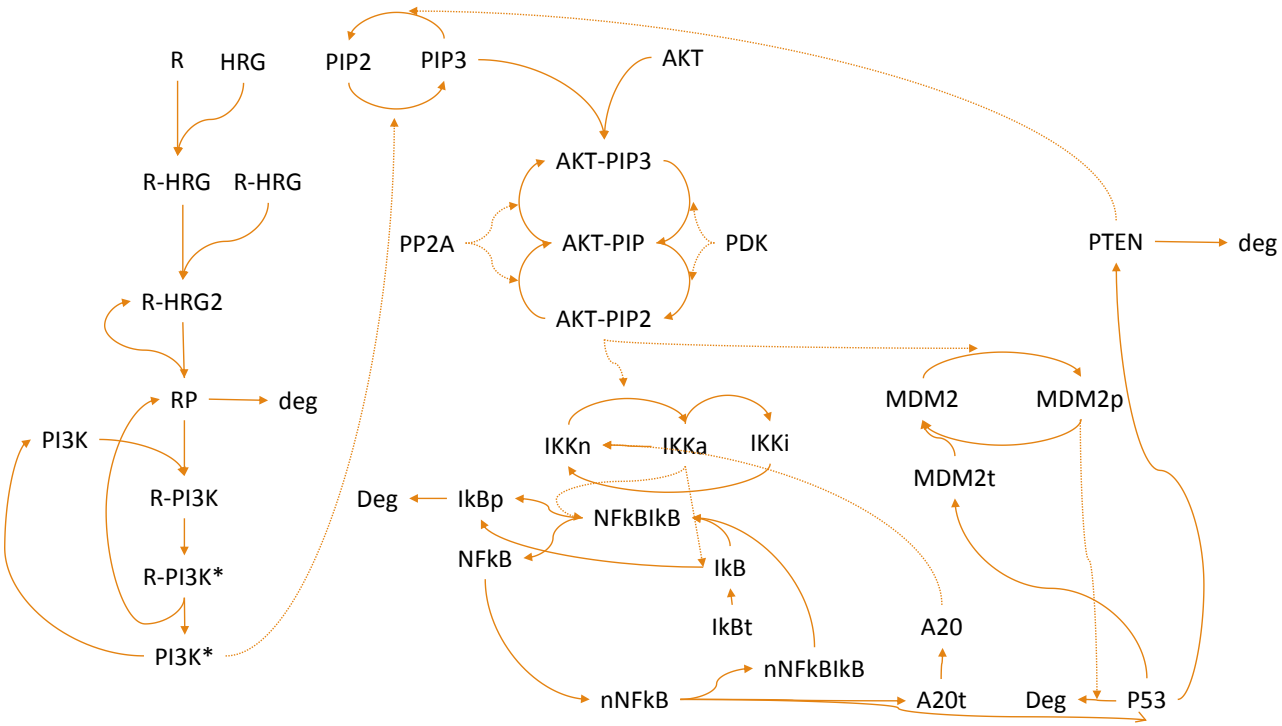

Figure 5 Diagrammatic representation of the combined model of the NFkB pathway.

Initial conditions

Table 6 Initial conditions for the simulation of the Combined model

Species	Value	Units
NFkB_IkBa	0.16	µM
ErbB4_R	0.08	µM
HRG	0.01	µM
PI3K_1	0.01	µM
AKT	0.01	µM
PP2A	1.14E-5	µM
PIP2	0.08	µM
MDM2t	0.0080	µM
MDM2p	0.016	µM
P53	0.016	µM
MDM2	0.0080	µM

Sensitivity analysis:

In order to obtain the desired time course profiles with the model sensitivity analysis was performed and, used in order to existing experimental data of time course profiles.
Sensitivity analysis data is present in the appendix.

Model validation:

In order to validate the model we aimed to match our time course profile with that of Total NFkB profile obtained through western blotting (1).

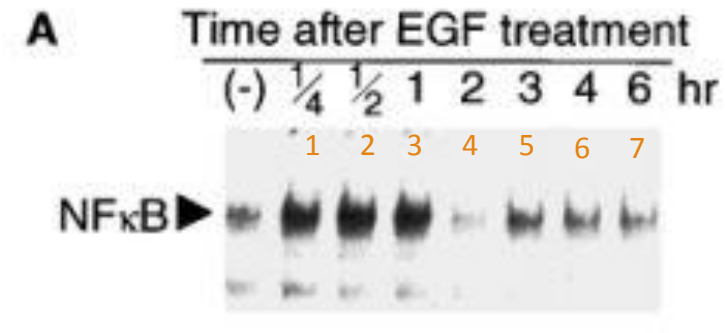

Figure 6 Western blot of a time course profile of Total NFkB for 6 hours (1)

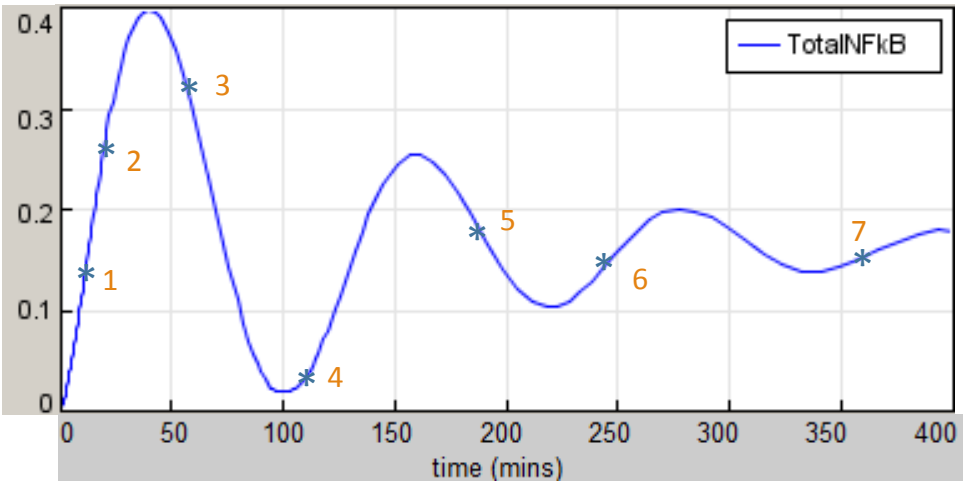

Figure 7 Time course simulation of the combined model of TotalNFkB for the duration of 400 minutes

The time course profile had similar behaviour to that seen in the western blot data, with an increase at ¼, ½ and, high TotalNFkB at 1 hour with a significant decrease by 2 hours and maintaining a relatively steady state through oscillations at 3, 4 and, 5 hours.

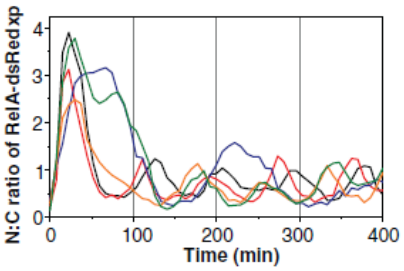

Figure 8 Nucleus to cytoplasm ratio of Rel A-dsRedxp as shown in the Ashall model (2)

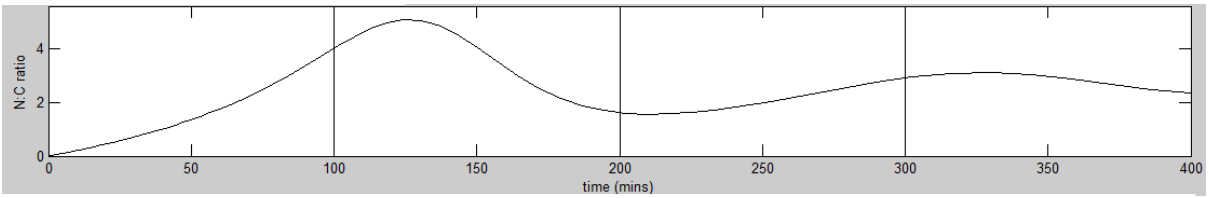

Figure 9 Nucleus to cytoplasm ratio of NFkB as obtained with the combined model.

For further validation we attempted to match the Nucleous:cytoplasm ratio presented in the Ashall model (2). The value obtained of 5 N:C ratio closely matched the N:C ratio peak of 4 shown in the Ashall model.

Discussion

At the end of rotation one, creating an *in silico* model of the NFkB pathway and, providing a link with the BTK pathway was achieved with relative success. However further validation and reduction in the reliance of parameter estimation is required though wet lab experimentation.

In order to improve the mathematical model besides the wet lab parameter estimation, different approaches to modelling could be used to improve the current model. As an alternative to using the Hill equation, Sequential binding could be used, thus allowing the addition of effectors and therefore transcriptional repressors or activators for the P53 and A20 modules in the model. Limitations of Michaelis-Menten kinetics also affect the validity of the model, as it is derived for isolated enzyme reactions. It raises issues of whether it remains sufficiently valid when extrapolated into a large reaction network or a multiple cell system. In natural conditions, steady state is not the norm and the reactants may be affected my perturbations or oscillatory inductions. Further issues arise when describing processes such as mRNA transcription since Hill kinetics and Michaelis-Menten kinetics were derived in the context of enzymatic reactions. This is because gene transcription is a multi-step process that utilizes molecular machinery at multiple levels (22).

Conclusion

In its current state, the model is able to describe the time-course profiles of NFkB signalling pathway enzymes, however further validation is required, additional parameters and, signalling modules related to the Bruton's tyrosine kinase pathway in order to be able to have a fully functional, KO and wild-type *in silico* model for the drug Ibrutinib.

Acknowledgements

I would like to thank Dr Steven Webb and Dr Ian Sorrell for their continuing support during this rotation.

References

1. Ohtsubo M, Takayanagi A, Gamou S, Shimizu N. Interruption of NF kappa B-Stat1 signaling mediates EGF-induced cell-cycle arrest. J Cell Physiol. 2000;184(1):131-7.
2. Ashall L, Horton CA, Nelson DE, Paszek P, Harper CV, Sillitoe K, et al. Pulsatile Stimulation Determines Timing and Specificity of NF-kappa B-Dependent Transcription. Science. 2009;324(5924):242-6.
3. Advani RH, Buggy JJ, Sharman JP, Smith SM, Boyd TE, Grant B, et al. Bruton tyrosine kinase inhibitor ibrutinib (PCI-32765) has significant activity in patients with relapsed/refractory B-cell malignancies. Journal of clinical oncology : official journal of the American Society of Clinical Oncology. 2013;31(1):88-94.

4. MacEwan DJ, Bowles KM, Rushworth SA. Emerging Therapy Targeting Tyrosine-Protein Kinase Btk: Potential for Ibrutinib and Other Btk Inhibitors. Drug Future. 2013;38(8):569-73.
5. Senior K. Positive results for ibrutinib in B-cell malignancies. Lancet Oncol. 2012;13(12):E522-E.
6. Ghosh S, Karin M. Missing pieces in the NF-kappaB puzzle. Cell. 2002;109 Suppl:S81-96.
7. Oeckinghaus A, Hayden MS, Ghosh S. Crosstalk in NF-kappaB signaling pathways. Nat Immunol. 2011;12(8):695-708.
8. Lin A, Karin M. NF-kappaB in cancer: a marked target. Seminars in cancer biology. 2003;13(2):107-14.
9. Basak S, Hoffmann A. Crosstalk via the NF-kappaB signaling system. Cytokine & growth factor reviews. 2008;19(3-4):187-97.
10. Kurzrock R, Estrov Z, Ku S, Leonard M, Talpaz M. Interleukin-1 increases expression of the LYT-10 (NFkappaB2) proto-oncogene/transcription factor in renal cell carcinoma lines. The Journal of laboratory and clinical medicine. 1998;131(3):261-8.
11. Lipniacki T, Paszek P, Brasier AR, Luxon B, Kimmel M. Mathematical model of NF-kappaB regulatory module. Journal of theoretical biology. 2004;228(2):195-215.
12. Bhalla US, Iyengar R. Emergent properties of networks of biological signaling pathways. Science. 1999;283(5400):381-7.
13. Michaelis L, Menten ML. The kinetics of the inversion effect. Biochem Z. 1913;49:333-69.
14. Briggs GE, Haldane JB. A Note on the Kinetics of Enzyme Action. The Biochemical journal. 1925;19(2):338-9.
15. Barcroft J, Hill AV. The nature of oxyhaemoglobin, with a note on its molecular weight. The Journal of physiology. 1910;39(6):411-28.
16. Rossi FM, Kringstein AM, Spicher A, Guicherit OM, Blau HM. Transcriptional control: rheostat converted to on/off switch. Molecular cell. 2000;6(3):723-8.
17. Alon U. An introduction to systems biology : design principles of biological circuits. Boca Raton, Fla. ; London: Chapman & Hall/CRC; 2006. xvi, 301 p. p.
18. Ferrell JE, Jr., Machleder EM. The biochemical basis of an all-or-none cell fate switch in Xenopus oocytes. Science. 1998;280(5365):895-8.
19. Holt JM, Ackers GK. The Hill Coefficient: Inadequate Resolution of Cooperativity in Human Hemoglobin. Method Enzymol. 2009;455:193-212.
20. Gong HJ, Zuliani P, Komuravelli A, Faeder JR, Clarke EM. Analysis and verification of the HMGB1 signaling pathway. Bmc Bioinformatics. 2010;11.
21. Hatakeyama M, Kimura S, Naka T, Kawasaki T, Yumoto N, Ichikawa M, et al. A computational model on the modulation of mitogen-activated protein kinase (MAPK) and Akt pathways in heregulin-induced ErbB signalling. The Biochemical journal. 2003;373(Pt 2):451-63.
22. Krebs JE. Lewin's genes XI. 11th / edited by Jocelyn E. Krebs, Stephen T. Kilpatrick, Elliott S. Goldstein. ed. Sudbury, Mass.: Jones and Bartlett; 2013. xxvii, 940 p p.